UNPUBLISHED PRELIMINARY DATA

N65-35267

[redacted]

39 p

$2.00 Hard Copy
$.50 Microfiche

[redacted]

NASA CW56920
Code 1
Cat 26

ABSTRACT

NSG-6-Rice

THE MEASUREMENT OF SUPERPARAMAGNETIC PARTICLE SHAPES AND SIZE DISTRIBUTION

by R. M. Asimow

The magnetization curves for specimens containing superparamagnetic particles are considered. It is shown that the curves may differ from a Langevin function because of particle anisotropy, particle interactions and because of the presence of a size distribution of particles. The various causes of particle anisotropy are considered, and magnetization curves for specimens with cubic and uniaxial anisotropy are presented. The magnetization curves depend on the sign of the anisotropy energy and in the case of a negative uniaxial anisotropy (prolate spheroids) the resulting curves may differ very considerably from a Langevin function.

A graphical technique is developed whereby it is possible to separate out the effects of the size distribution, the particle interaction and the particle anisotropy. Thus it is possible to obtain quantitative values for both the particle shape and the size distribution.

[redacted]

RC#7

THE MEASUREMENT OF SUPERPARAMAGNETIC PARTICLE SHAPES AND SIZE DISTRIBUTIONS

R. M. Asimow

Introduction

In the particle size range below 100Å it is quite difficult to obtain quantitative size and shape information on precipitate particles. All of the available techniques have their limitations; however, quantitative applications of superparamagnetism have not been developed as fully as possible due to a lack of analysis of the complete magnetization curve. With such an analysis it appears possible to obtain from a single magnetization curve of a specimen containing randomly oriented SPM (superparamagnetic) particles a quantitative volume distribution and a description of the particle shape.†

---

†A quantitative technique for determination of size distribution has been previously developed by Weil and Gruner.[1] Their technique is experimentally more difficult to apply than the one discussed in this paper as it requires magnetization measurements over a very large temperature interval. Furthermore, it is necessary to know the type of anisotropy and particle shape before it can be applied. In their application it has been assumed that at 0°K the specimen remnance is $R = 0.5I_o$ where I_o is the saturation magnetization. This is only true for prolate

spheroids, for other shapes and anisotropies different coefficients are required. As shown later in this paper, for flat oblate spheroids with a negative cubic crystalline anisotropy energy the appropriate constant is $1/\sqrt{2}$.

An isolated isotropic SPM particle should show a magnetization curve that can be expressed by a Langevin function[2]

$$I/I_s = \mathrm{ctnh}(HVI_s/kT) - kT/HVI_s \qquad [1]$$

where I_s is the saturation magnetization, V the particle volume, H the applied field, T the particle temperature, k the Boltzmann constant, and I the magnetization in the direction of the applied field. Such behavior is rarely if ever observed in actual systems. One explanation for this is that the SPM particles do possess a significant anisotropy and thus the magnetic energy associated with the particle depends on the direction of magnetization in a more complicated way than for the isotropic particle of Eq. [1].

In general the magnetic energy E of an isolated SPM particle embedded in a nonmagnetic matrix can be expressed as a sum of several contributions.

$$E = E_h + E_d + E_s + E_c \qquad [2]$$

where E_h is the external field energy, E_d the energy resulting from the particle demagnetizing factor, E_s the magnetostriction energy, and E_c the crystalline anisotropy energy. In each term

we consider only the part dependent on the orientation of the magnetization vector and the particle axes as the shape of the magnetization curve will be determined by these contributions. Following the same procedure used in deriving the Langevin function, we can write for a collection of noninteracting randomly oriented particles in thermal equilibrium

$$\frac{I}{I_o} = \frac{1}{4\pi}\int_0^{2\pi} d\theta \int_0^{\pi} \sin\alpha d\alpha \; \frac{\int_0^{2\pi} d\omega \int_0^{\pi} \cos\phi \sin\phi \; \exp[-E(\phi,\alpha,\omega,\theta,\eta)/kT] d\eta}{\int_0^{2\pi} d\omega \int_0^{\pi} \sin\phi \; \exp[-E(\phi,\alpha,\omega,\theta\eta)/kT] d\eta} \qquad [3]$$

where I_o is the saturation magnetization of the specimen and the angles are defined in Fig. 1. In order to predict the magnetization curve we have to evaluate $E(\phi,\alpha,\omega,\theta,\eta)$ where ϕ is a function of the other angles, and carry out the integration. We start by looking at each of the terms in Eq. [2].

Field Energy

$$E_h = -HVI_s\cos\phi \qquad [4]$$

Demagnetizing Energy

In order to obtain a fairly simple expression for this term we will consider only particles which are ellipsoids of revolution and thus have uniaxial anisotropy. The angular

dependent part of the demagnetizing energy is given by[3]

$$E_d = \pi V I_s^2 [(3N/4\pi) - 1] \cos^2 \eta \qquad [5]$$

where N is the demagnetizing factor along the principal axis. This term will be positive for oblate spheroids and negative for prolate spheroids.

Crystalline Anisotropy Energy

Most of the SPM particles studied have cubic crystal structure so we can write, neglecting higher order terms[4]

$$E_c = KV(n_1^2 n_2^2 + n_2^2 n_3^2 + n_3^2 n_1^2)$$

where the n_i are direction cosines and K is the anisotropy constant. In terms of the angles defined in Fig. 1, this equation can be written as

$$E_c = KV(\sin^4 \eta \sin^2 2\omega + \sin^2 2\eta)/4 \qquad [6]$$

This term may be positive or negative depending on the sign of K.

Magnetostriction Energy

To evaluate this term in a straightforward manner we make several additional assumptions; the SPM particles have isotropic magnetostriction and elastic constants, the elastic constants are identical with those of the matrix and the particle has a lattice similar to and is coherent with the matrix.† Thus, if

†From a theoretical point of view, the only restriction

required on the elastic constants is that the matrix be elastically isotropic; however, the calculations become exceedingly laborious unless the additional restrictions are imposed.

---

it were not for the constraining effect of the matrix and the magnetostriction strains, the region of the specimen which becomes the particle would undergo a homogeneous dilatation. Due to the coherency strains, there is strain energy present in both the particle and the matrix.

For the unconstrained particle we can write the transformation strains e^T_{ij} on formation of the particle as

$$e^T_{ij} = e^\circ \delta_{ij} + e^\pi_{ij}$$

where e° is the magnitude of the hydrostatic strain, δ_{ij} is a Dirac delta function and e^π_{ij} are the magnetostriction strains. In terms of the angles defined in Fig. 1, the magnetostriction strains are given by equations of the type[4]

$$e^\pi_{33} = (3\gamma/2)\,(\cos^2\eta - \tfrac{1}{3})$$

where γ is the isotropic magnetostriction constant and e^π_{33} is the normal strain along the polar axis.

Eshelby has shown that the strain energy of the particle and matrix is

$$E_{elas} = -(V/2)p^I_{ij}e^T_{ij}$$

where p^I_{ij} are the homogeneous stresses in the particle.[5,6] He has further derived the formulae necessary for calculation of p^I_{ij}. The strains in the particle due to the constraint of the surrounding matrix are given by

$$e^C_{ij} = S_{ijkl}\, e^T_{kl}$$

where the S_{ijkl} can readily be calculated in terms of the demagnetizing factors of the particle. The stresses in the particle are then calculated from the relation

$$p^I_{ij} = \lambda(e^C - e^T)\delta_{ij} + 2\mu(e^C_{ij} - e^T_{ij})$$

where e^C and e^T are the scalar parts of e^C_{ij} and e^T_{ij}, and λ and μ are the Lame elastic constants. Using these results and assuming $e^\pi_{ij} \ll e^\circ$, we can express the angular dependent part of the elastic strain energy as

$$E_s = \frac{3}{8}\, Ve^\circ\gamma\mu\left(\frac{1-2\zeta}{1-\zeta}\right)\left(\frac{3N}{4\pi} - 1\right)\cos^2\eta \qquad [7]$$

where ζ is Poisson's ratio. This term will be either positive or negative depending on the sign of $e^\circ\gamma$, and the particle shape.

These results need perhaps a small amount of explanation

in view of the fact that it has been recently stated in an analysis of a somewhat similar problem that magnetostriction can never give rise to uniaxial anisotropy in coherent precipitates in FCC metals.[7] If an ellipsoidal region on transforming to a particle undergoes a homogeneous dilatation only, then the strain energy is independent of particle shape.[8] We now add small additional strains due to magnetostriction and find that the change in strain energy of the system depends on the initial shape of the ellipsoid and on the orientation of the magnetostriction strains with respect to the ellipsoid. The result shows that the strain energy of the system is minimized if the magnetostriction strain is of the opposite sign as the transformation strain along the short axes of the particle.

Magnetization Curves of Anisotropic Particles

On reviewing the various energy terms, we see that both E_s and E_d exhibit uniaxial anisotropy whereas E_c has a cubic symmetry. In order to simplify the calculation of magnetization curves it is convenient to consider the two types of symmetry separately. First we consider the solution to Eq. [3] for a system of particles possessing crystalline anisotropy only. The required integration must be carried out numerically and the results can be expressed in terms of two dimensionless energy parameters

$$I/I_o = f(HI_sV/kT,\ KV/kT) \qquad [8]$$

Magnetization curves for positive values of KV/kT are shown in Fig. 2a, and for negative values of KV/kT in Fig. 2b. If the particles are to be in fact SPM, then upper and lower limits exist for KV/kT since the energy barrier for magnetization reversal cannot exceed about 20kT.[2] For negative K, the energy barrier for rotation from one <111> direction to another is K/12 and for positive K the barrier for rotation from a <100> direction to another is K/4 (reference 4 Fig. 12-24). Thus it follows that $-240 < KV/kT \lesssim 80$. From Fig. 2a and 2b it is seen that for $-10 < KV/kT < 5$ there is a negligible deviation of the magnetization curve from that of a Langevin function. Thus for temperatures greater than about $24T_h$ where T_h is the lowest temperature at which no hysteresis is observed in the magnetization curve, it is certainly safe to neglect the effect of cubic anisotropy.

Looking at the uniaxial energy terms, we have

$$E_d + E_s = E_u \cos^2\eta \qquad [9]$$

where

$$E_u = \pi V[I_s^2 - \frac{3\mu}{8\pi}e^{\circ}\gamma(\frac{1-2\zeta}{1-\zeta})\ (\frac{3N}{4\pi} - 1)] \qquad [10]$$

If E_u is negative, the energy minimum, in the absence of an applied field, occurs along the particle polar axis and the

energy barrier to magnetization reversal is given simply by E_u. On the other hand, if E_u is positive then the energy minimum occurs at the particle equator and there is no energy barrier. Thus the limits on E_u for SPM behavior are $-20<E_u/kT<\infty$. In order to obtain magnetization curves with E_u/kT as a parameter, it is again necessary to resort to numerical integration. A series of such curves are shown in Fig. 3a for positive E_u and in Fig. 3b for negative E_u. It is of interest to note that as pointed out by Bean[9] the limiting slope as $H \to 0$ is independent of the anisotropy term in both Figs. 2 and 3. In the case of extremely large negative anisotropies (very large needle-like particles) each particle acts like a quantum moment of spin 1/2 in that the magnetization vector is either parallel or antiparallel to the particle axis.[9] In this limiting case the magnetization can be obtained by a simple series expansion and the result is shown for comparison in Fig. 3b. For very large positive anisotropies (large plates), it is easy to show that at high fields the limiting magnetization is $\pi/4$ and this value is shown in Fig. 3a.

In sufficiently high fields the saturation magnetization is unaffected by particle shape; however, as seen in Fig. 4, the approach to saturation may be very slow for highly anisotropic particles and the use of the limiting slope on a 1/H plot to determine an average particle size as suggested by Cahn can lead to considerable error in these cases.[10] In both Figs. 2 and 3, at intermediate fields increasing deviations

from Langevin behavior are exhibited as the anisotropy increases and for either types of anisotropy considered separately we can write

$$I/I_o = f(F,S) \qquad [11]$$

where S is a dimensionless anisotropy energy and F is the dimensionless field energy (HI_sV/kT). In most cases where the particle shape differs significantly from a sphere, the uniaxial anisotropy term causes considerably greater deviations from the Langevin function than the cubic term. In the rest of this paper, we will neglect the cubic term and assume only uniaxial anisotropy to be present.

Particle Size Distribution and Specimen Magnetization Curves

An additional explanation for experimentally observed non-Langevin curves lies in the fact that invariably particles present in any specimen cover some size distribution.† Thus,

†This problem has been partially considered by Kneller and others who have considered the effect of a distribution in size of isotropic SPM particles.[11]

at any applied field, particles of different size will have a different average magnetization since both F and S are directly proportional to volume. In order to solve this problem we will assume that the actual geometric shape of all particles is identical but that the particle volumes follow a logarithmic

normal distribution†

$$P(v) = (1/2\pi\sigma^2)^{1/2} \exp[-(\ln V - \ln V_o)^2/2\sigma^2] \qquad [12]$$

---

†This assumption is certainly arbitrary, but in order to utilize a distribution function with more than two adjustable parameters, exceedingly accurate magnetization versus field measurements are required and the theory would have to be correspondingly refined.

---

where σ is the variance of the distribution and $\ln V_o$ is the mean logarithmic particle volume. Three parameters then completely represent the system of particles (N, V_o and σ) and three pieces of experimental data are necessary to obtain them. To see how this may be accomplished, consider the schematic magnetization curve shown in Fig. 5. From the analysis by Cahn[10] it is easy to show that on defining an H_L as shown we have the relation

$$HI_s(\overline{V^2}/\overline{V})/kT = 3H/H_L \qquad [13]$$

where $\overline{V^2}$ is the mean squared particle volume and $\overline{V}$ is the mean particle volume ($\overline{V} \neq V_o$ unless $\sigma = 0$). This statistic is independent of any assumption regarding the distribution function of particle sizes and is also independent of particle shape. In order to obtain two other pieces of information we arbitrarily choose fractional magnetizations of $I/I_o = 0.5$

and $I/I_o = 0.85$ and determine the corresponding applied fields. By combining Eqs. [11] and [12] we obtain

$$\frac{I(\bar{F},\bar{S},\sigma)}{I_o} = \int_0^\infty P(V)\ \frac{I(F,S,\sigma)}{I_o}\ dV \qquad [14]$$

where it is to be remembered that F and S are proportional to V, and $\bar{F}$ and $\bar{S}$ are the values of F and S calculated using the mean particle volume. For a logarithmic normal distribution the following relations exist

$$\bar{V} = V_o \exp(\sigma^2/2) \qquad [15a]$$

$$\overline{V^2}/\bar{V} = V_o \exp(\sigma^2) \qquad [15b]$$

We can thus express σ in terms of $3H/H_L$ and V_o. Given I/I_o, we can eliminate V_o and write

$$I/I_o = .5 = g_1(3H/H_L,\bar{F},\bar{S}) \qquad [16a]$$

$$I/I_o = .85 = g_2(3H/H_L,\bar{F},\bar{S}) \qquad [16b]$$

On numerically solving [16] we obtain the curves shown in Figs. 6 and 7 which may be used to determine N, σ, and V_o for any specimen containing uniaxial SPM particles in the following way. From experimental data, $3H/H_L$ is known for $I/I_o = 0.5$ and 0.85. Thus one knows which curve in either Figs. 6a and 6b (oblate spheroids) or Figs. 7a and 7b (prolate spheroids) corresponds to the specimen but one does not know

the location on the curve. However, the ratio of the two applied fields H(.5)/H(.85) is known experimentally and thus all that is necessary is to determine which pair of points on the two curves have the same ordinates and have abscissa which are in the above ratio. Then S_o and $\overline{F}$ can be read off either curve and $\overline{V}$, $\overline{S}$, σ and N calculated from the relations

$$\overline{V} = \overline{F}kT/HI_s \qquad [17a]$$

$$\overline{S} = S_o \exp(\sigma \frac{2}{2}) \qquad [17b]$$

$$\sigma = [2 \ln(\frac{3H}{H_L\overline{F}})]^{\frac{1}{2}} \qquad [17c]$$

$$N = \frac{4\pi}{3}\left\{ \frac{\overline{S}kT}{\pi\overline{V}} [I_s^{\,2} + \frac{3}{8\pi}(\frac{1 - 2\zeta}{1 - \zeta})\mu e^{\circ}\gamma]^{-1} + 1\right\} \qquad [17d]$$

One ambiguity arises in this procedure: in order to know whether to use Figs. 6a and 6b or Figs. 7a and 7b it is necessary to know if E_u is positive or negative, that is if the particles are oblate or prolate spheroids. This problem can be resolved by some additional information such as electron microscopy or by a determination of T_h. From T_h, the anisotropy energy can be calculated and thus the type of particle anisotropy can be determined.

Particle Interactions

One additional cause of non-Langevin behavior must be considered. If the concentration of SPM particles is high enough

there may be significant particle interactions so that the system as a whole possesses a Curie temperature. This possibility can be readily checked experimentally since as previously pointed out the initial slope of the magnetization curve is unaffected by particle anisotropy. Thus if magnetic measurements are made at two or more temperatures, the reciprocal of the initial susceptibility when plotted versus the absolute temperatures should intercept the origin if the interactions are negligible. If the intercept is not at the origin but indicates a Curie temperature θ then from the simple Weiss theory the particle interactions may be taken into account. It follows from this theory that the magnitude of the internal field is given by NI where

$$N = \theta/\chi_T(T - \theta) \qquad [18]$$

and χ_T is the initial susceptibility at temperature T ($\chi_T = I_o/H_L$). Thus provided the magnetization curve is measured at a temperature greater than θ all the previous discussion is still valid provided that the experimental curve is simply replotted against H + NI rather than versus H.

If the measurement temperature is below θ then the magnetization curve should exhibit remanence which points out the interesting fact that there are two possible causes of hysteresis in SPM specimens. Barring the formation of a sort of super

domain structure (domains formed from many SPM particles) this latter type of hysteresis curve should show a discontinuity in I for fields in the neighborhood of the coercive force. Because the coercive force is a function of particle size; in an actual specimen such a discontinuity would not be observed.

Experimental Procedure

A Au - 8.73 at pct Co polycrystalline sheet specimen 0.011 in. thick and about 1/2 in. square was used for the experimental work. After solution treating at 982°C for one hour in vacuum, the specimen was water quenched and aged for various times at 202°C. Magnetization measurements were made at 77°K in fields up to 10,000 oersteds and at 298°K in fields up to 16,000 oersteds using a Foner[12] type magnetometer. Magnetization curves for a specimen aged 6,635 minutes are shown in Fig. 8. From a plot of reciprocal susceptibility versus temperature it was found that $\theta = 20°K$. In determining further parameters from the magnetization curves the appropriate correction according to Eq. [18] was used. On the scale of Fig. 8 this correction is not detectable.

In order to calculate N from Eq. [17d] the numerical values listed in Table I have been used. The quantity which involves the greatest uncertainty is γ as there is no direct measurement on FCC Co. Fortunately the final calculation of particle eccentricity is not sensitive to γ as the magneto-

striction energy is considerably smaller than the demagnetizing energy. Another estimate of γ can be obtained from the work of Rodbell[14] who determined the quantity $d \ln K / d e^{\circ} = 4.1$. This result coupled with the analysis of Kittel[18] and assuming elastic isotropy yields a value of $\gamma = -1.8 \times 10^{-6}$. The value listed in the table has been used in the calculations. For the quantity which involves elastic constants, the average of the result for Au and for Co is used. Inserting these values in Eq. [17d] we find

$$N = (4\pi/3)\ [1.55 \times 10^{-7} kT(\overline{S}/\overline{V}) + 1]$$

Table I. Values of Physical Parameters for Au-Co Specimens

Quantity	Value	Comments	Reference
I_s	1422 cgs	value for bulk HCP Co at 20°C there appears to be little difference between saturation value for FCC and HCP Co and also the value appears to be nearly independent of size down to very small sizes (see ref. 13)	4(p. 867)
ζ_{Au}	0.42		15(p. 614)
ζ_{Co}	0.32	value for HCP polycrystalline material	16(p. 109)
μ_{Au}	$.28 \times 10^{12}$ dynes/cm^2	computed from values of elastic constants for polycrystalline Au at 20°C	15(p. 614)
μ_{Co}	$.81 \times 10^{12}$ dynes/cm^2	computed from values of elastic constants for polycrystalline HCP Co at 20°C	16(p. 108)
$e°$	-0.14	obtained from difference in lattice parameters of FCC Co and Au	17(p. 646)
γ	-10×10^{-6}	obtained from measurements on FCC Co particles in Cu	7

Previous work using electron microscopy has indicated that the precipitate in this system is essentially platelike and thus Fig. 8 was analyzed in conjunction with Figs. 6a and 6b.[19] Using Eqs. [17a,b,c and d] the results shown in Table II were obtained.

Table II. Results of Magnetic Analysis

Temperature °K	S_o	$\bar{S}$	$\bar{V}$ $ccx10^{21}$	$N/4\pi$	σ
77	14	25	29.1	.96	1.07
298	9	11.8	21.7	1.17	.74

Discussion

The comparison of results obtained at two different temperatures should be a sensitive test for the validity of the analysis. It can be seen in Table II that the values of $\bar{V}$, $N/4\pi$, and σ which should be identical for the two temperatures agree within about $\pm$ 15%. Probably the most important reason for the lack of better agreement is the difficulty in obtaining an accurate value of the saturation magnetization. No doubt, the use of higher fields would greatly alleviate this problem. The procedure adopted for determining the saturation magnetization is shown in Fig. 9. Two extrapolation techniques were used: (1) the final experimental slope was extrapolated to infinite field and (2) after roughly determining the particle size, the limiting slope neglecting particle anisotropy (Cahn analysis) was drawn in from the highest attainable experimental field. The average of the two extrapolated values was used.

While it might seem that the agreement between the two temperatures is not particularly good, it should be pointed out that the values of $\bar{V}$ calculated using the present procedure are an order of magnitude larger than those obtained by simple extrapolation of the final experimental slope. The maximum meaningful value for $N/4\pi$ is one, corresponding to a completely flat oblate spheroid. Within the experimental accuracy it must be concluded then that the particles are essentially disks which confirms the analysis by Gaunt. Unfortunately in this system, the magnetic analysis could not be extended over a large range of aging times; at shorter times the uncertainty in the saturation magnetization was too great whereas at longer times hysteresis appeared in the magnetization curve at 77°K so that it was not possible to determine a Curie temperature.

Gaunt has already speculated on the reasons for the large remanence and coercive force observed in the Au-Co system.[20] In view of the additional information gained from the present investigation some additional comments can be made. Gaunt has observed that the ellipsoid axes of the particles are coincident with the <100> directions. Thus for a stable single domain particle, on reducing the magnetic field after saturation, the magnetization vector rotates to the lowest energy

position in the equatorial plane of the oblate spheroid. This is the <110> axis nearest the magnetic field vector for negative crystalline anisotropy. In this case it can be shown that the remanence for a random array of stable single domain particles is given by

$$R = I_o/\sqrt{2}$$

If an oblate spheroid is to be stable, then the energy barrier for rotation of the magnetization vector in the equatorial plane (KV/4) must exceed 20kT. Thus $V > -80kT/K = 0.773 \times 10^{-18}$cc at 77°K ($K = -1.1 \times 10^6$ from the work of Bean[13] and Rodbell[14]). For particles which were aged longer times, it was attempted to explain the remanence at 77°K on this basis, assuming that the Curie temperature did not change. $\overline{V}$ and σ were obtained from the 298°K magnetization curve and thus the fraction of stable single domain particles at 77°K could be calculated. It was found that the remanence predicted on this basis was far less than that experimentally observed. This tends to confirm Gaunt's conclusion that strong particle interactions are responsible for the remanence. On the other hand this does not appear to be the entire answer since even in the magnetization curves shown in Fig. 8 there is a very small amount of remanence at 77°K and yet the Curie temperature is well below 77°K.

It is of interest to note that in the Cu-Co system most observers have concluded that, in the absence of aging in a magnetic field, the as aged SPM particles are nearly spherical in shape.[20] The anisotropies determined from these particles by various techniques are consistent with the crystalline anisotropy of FCC Co.[13,14] It has also been observed by Becker and others that magnetization curves taken at different temperatures superimpose very well when plotted against H/T. In fact this has been suggested as a criterion for SPM.[21] Actually, however, if anisotropy is important, then one should not expect this superposition, but, in fact, at high fields a low temperature curve should fall below a high temperature one on an H/T plot. This follows since the parameter S is independent of applied field and inversely proportional to T. Thus at constant H/T and decreasing T, the effect is to go to larger absolute values of S at constant F which invariably causes I/I_o to decrease. In the Cu-Co system, calculation shows that for crystalline anisotropy only, $T_h = 20°K$ for a particle of 50Å radius. Thus for the work reported in the literature where H/T superposition was observed, the measurement temperatures were sufficiently above T_h so that anisotropy was of negligible importance. In contrast, in the present investigation, where uniaxial anisotropy was the dominant term, SPM behavior was

observed (no hysteresis in the magnetization curves) and yet H/T superposition did not exist (see Fig. 8).

Acknowledgment

The author gratefully acknowledges the assistance of A. Ehlert who performed the experimental work. Support for this research was obtained through the National Aeronautics and Space Administration, Grant No. NsG-6-59.

References

[1]Louis Weil and Lucie Gruner: Comptes rendus, 1956, vol. 243, pp. 1629-1631

[2]J. J. Becker: Trans. Met. Soc. AIME, 1957, vol. 209, pp. 59-63

[3]E. C. Stoner and E. P. Wohlfarth: Trans. Roy. Soc. Lon., vol. A240, pp. 599-642

[4]R. M. Bozorth: Ferromagnetism, pp. 563, 634, D. Van Nostrand Co., Princeton, 1951

[5]J. D. Eshelby: Pro. Roy. Soc. Lon., 1957, Ser. A, vol. 241, pp. 376-396

[6]J. D. Eshelby: Pro. Roy. Soc. Lon., 1959, Ser. A, vol. 252, pp. 561-569

[7]C. W. Berghout: J. Phys. Chem. Solids, 1963, vol. 24, pp. 507-516

[8]F. R. N. Nabarro: Pro. Roy. Soc. Lon., 1940, Ser. A, vol. 175, pp. 519-538

[9]C. P. Bean: J. App. Phys., 1955, vol. 26, pp. 1381-1383

[10]John Cahn: Trans. Met. Soc. AIME, 1957, vol. 209, p. 1309

[11]Eckart Kneller: Z. fur Phys., 1958, vol. 152, pp. 574-585

[12]W. S. Foner: Rev. Sci. Inst., 1959, vol. 30, pp. 548-557

[13]C. P. Bean, J. D. Livingston and D. S. Rodbell: J. de Phys. et Rad., 1959, vol. 20, pp. 298-302

[14]D. S. Rodbell: J. Phys. Soc. Japan, 1962, sup. B-I, vol. 17, pp. 313-316

[15]C. J. Smithells: Metals Reference Book, 3rd. ed., vol. 2, p. 614, Butherworth and Co. Ltd., Washington, 1962

[16]Centre d'information du Cobalt: Cobalt Monograph, Brussels, 1960

[17]C. S. Barrett: Structure of Metals, 2nd ed., p. 646, McGraw-Hill Book Co., New York, 1952

[18]Charles Kittel: Rev. Mod. Phys., 1949, vol. 21, pp. 541-583

[19]P. Gaunt and J. Silcox: Phil. Mag., 1961, vol. 6, pp. 1343-1345

[20]P. Gaunt: Phil. Mag., 1960, vol. 5, pp. 1127-1145

[21]C. P. Bean, J. D. Livingston and D. S. Rodbell: Acta Met., 1957, vol. 5, pp. 682-684

[22]C. P. Bean and J. D. Livingston: J. App. Phys., 1959, sup. to vol. 30, pp. 120S-132S

Captions for Figures

Fig. 1 - The relative orientation of the applied magnetic field H, and the magnetization vector I with respect to the SPM particle axes N_1, N_2, N_3.

Fig. 2 - Dimensionless magnetization curves for specimens containing SPM particles with cubic anisotropy and random orientations. The anisotropy energy parameter VK/kT is positive in (a) and negative in (b).

Fig. 3 - Dimensionless magnetization curves for specimens containing SPM particles with uniaxial anisotropy and random orientations. The anisotropy energy parameter E_u/kT is positive in (a) and negative in (b).

Fig. 4 - Saturation magnetization curves for specimens with a negative uniaxial anisotropy.

Fig. 5 - Schematic magnetization curve showing definition of H_L and other important field values. Note that it is assumed by some extrapolation technique I_o is obtained.

Fig. 6 - Curves of $\bar{S}$ versus $\bar{F}$ with $3H/H_L$ as a parameter for oblate spheroids (E_u positive). (a) $I/I_o = .5$, (b) $I/I_o = .85$. Note that as $\bar{F}$ increases $\bar{S}$ also increases, that is for a constant magnetization as the anisotropy increases, the field also increases.

Fig. 7 - Curves of $\bar{S}$ versus $\bar{F}$ with $3H/H_L$ as a parameter for prolate spheroids (E_u negative). (a) $I/I_o = .5$, (b) $I/I_o = .85$.

Fig. 8 - Magnetization curves at 298°K and 77°K for a Au-Co specimen aged 6,635 min.

Fig. 9 - High field magnetization data plotted versus 1/H. The two extrapolation procedures used are shown. The dotted line shows the limiting slope calculated on the basis of the average particle volume and the dashed line is simply an extrapolation of the final experimental slope.

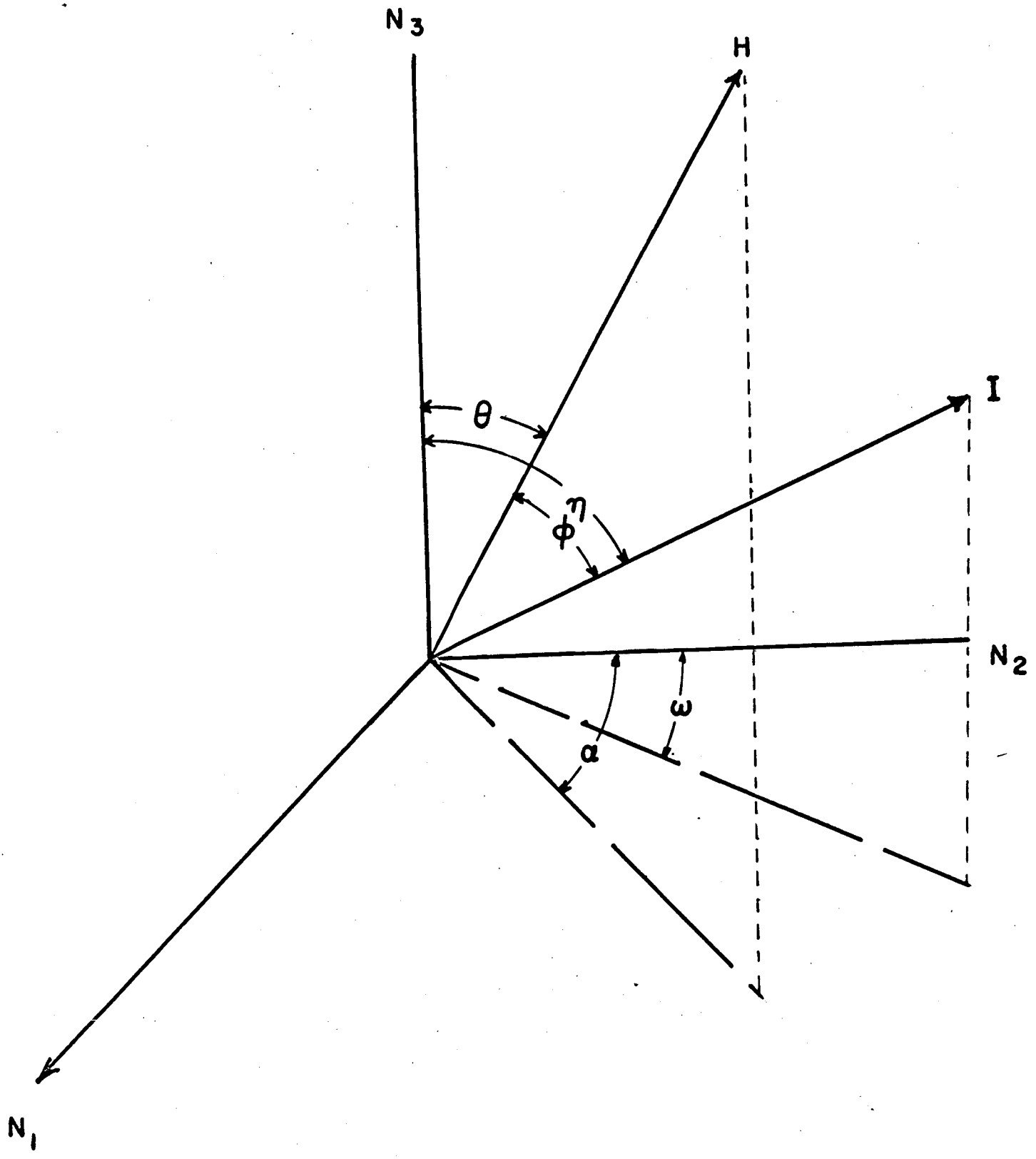
N3
H
I
θ
η
φ
N2
ω
α
N1

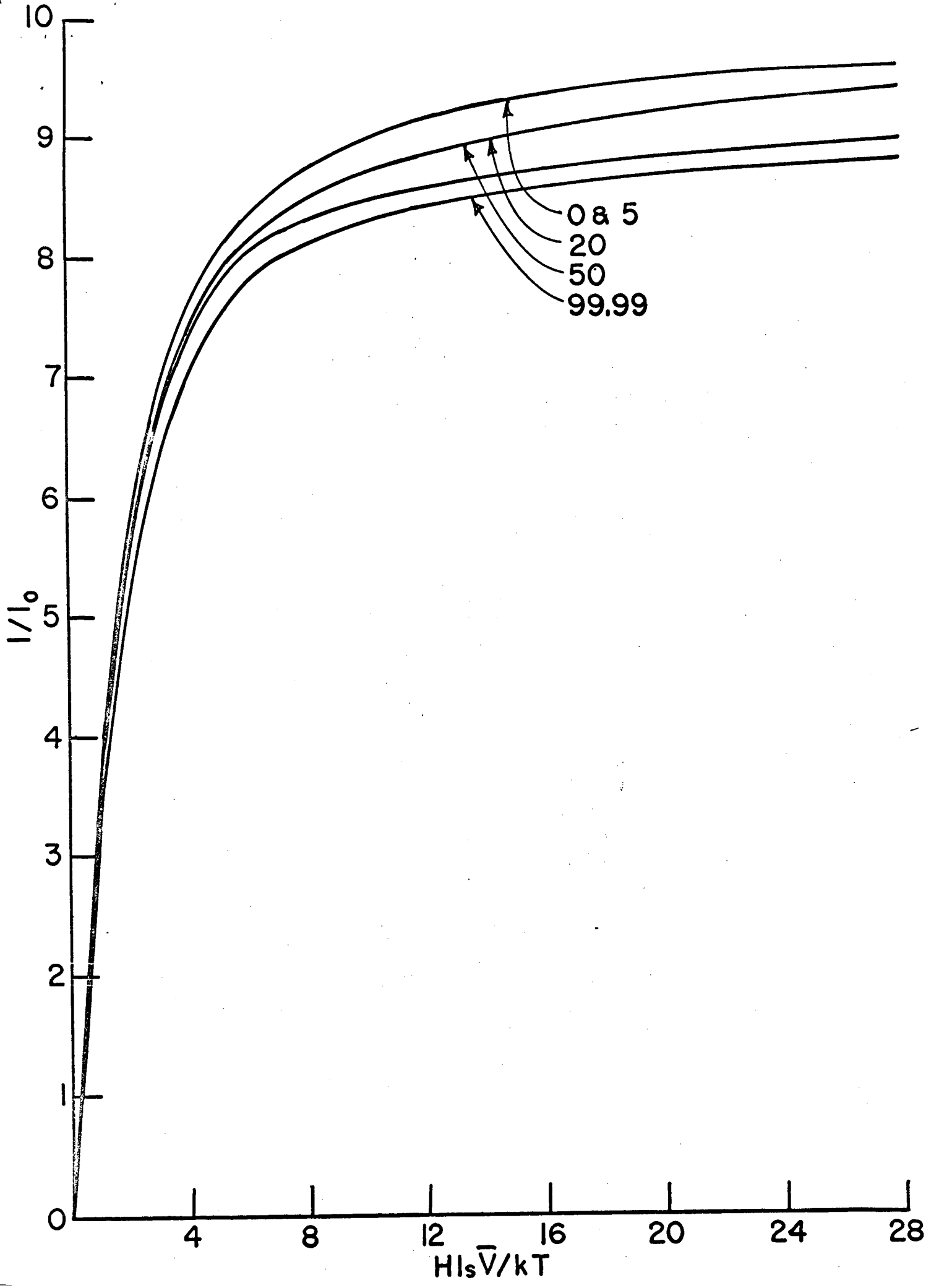
10
9
8
7
6
5
4
3
2
1
0
I/I_o
0 & 5
20
50
99.99
4
8
12
16
20
24
28
$HI_s\bar{V}/kT$

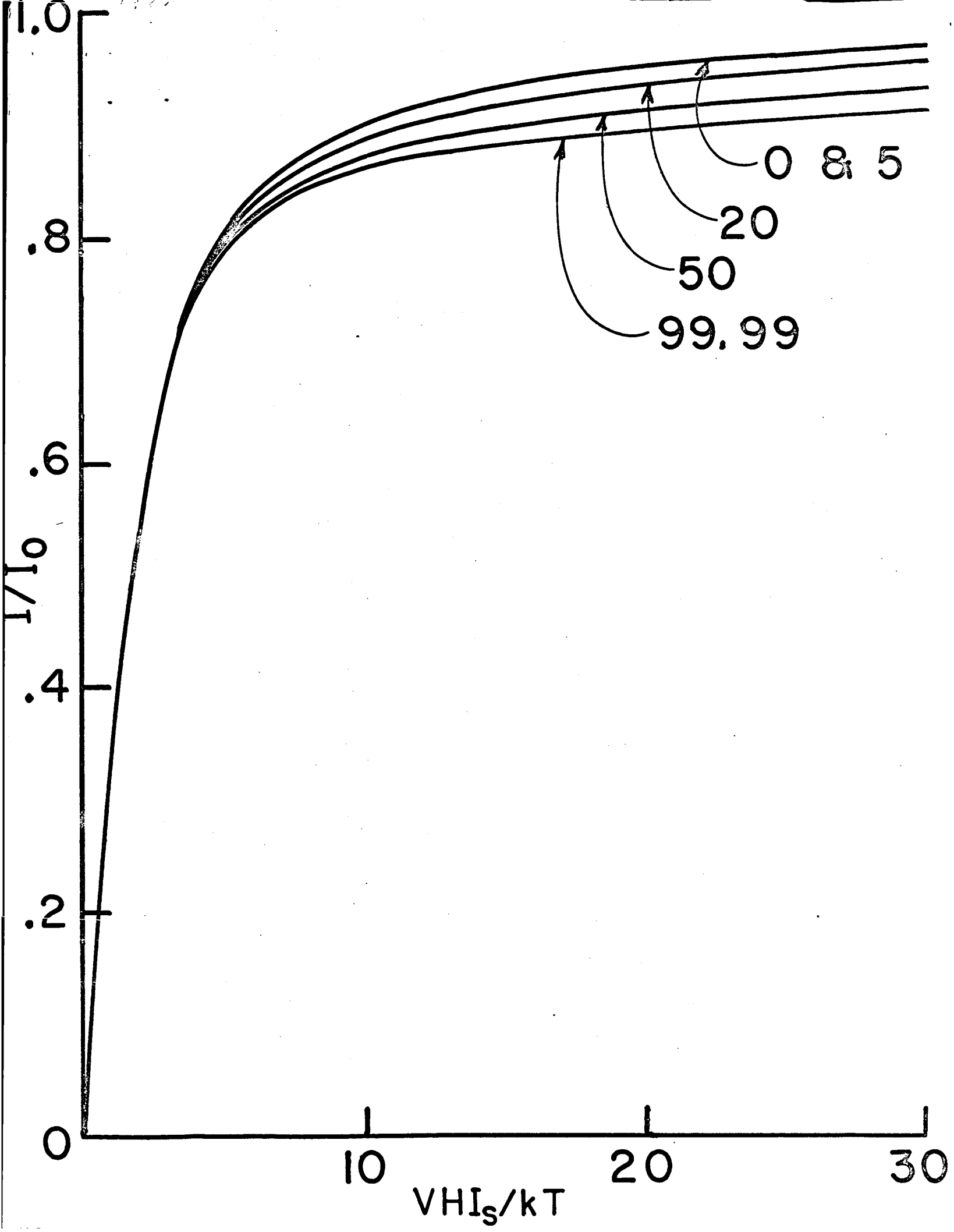
1.0
.8
.6
.4
.2
0
I/I_0
10
20
30
VHI_s/kT
0 & 5
20
50
99.99

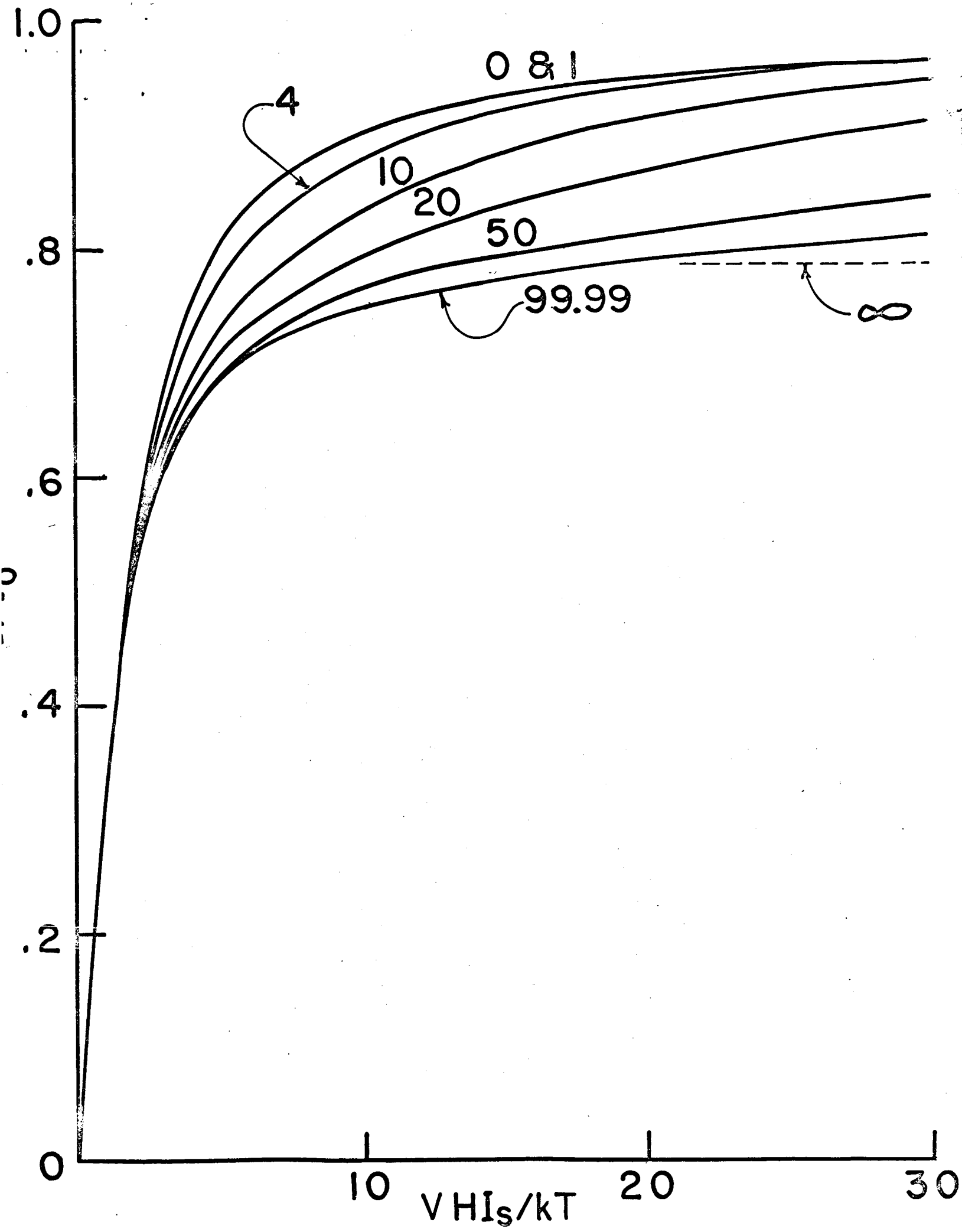
1.0
.8
.6
.4
.2
0
0 & 1
4
10
20
50
99.99
∞
10
20
30
VHIs/kT

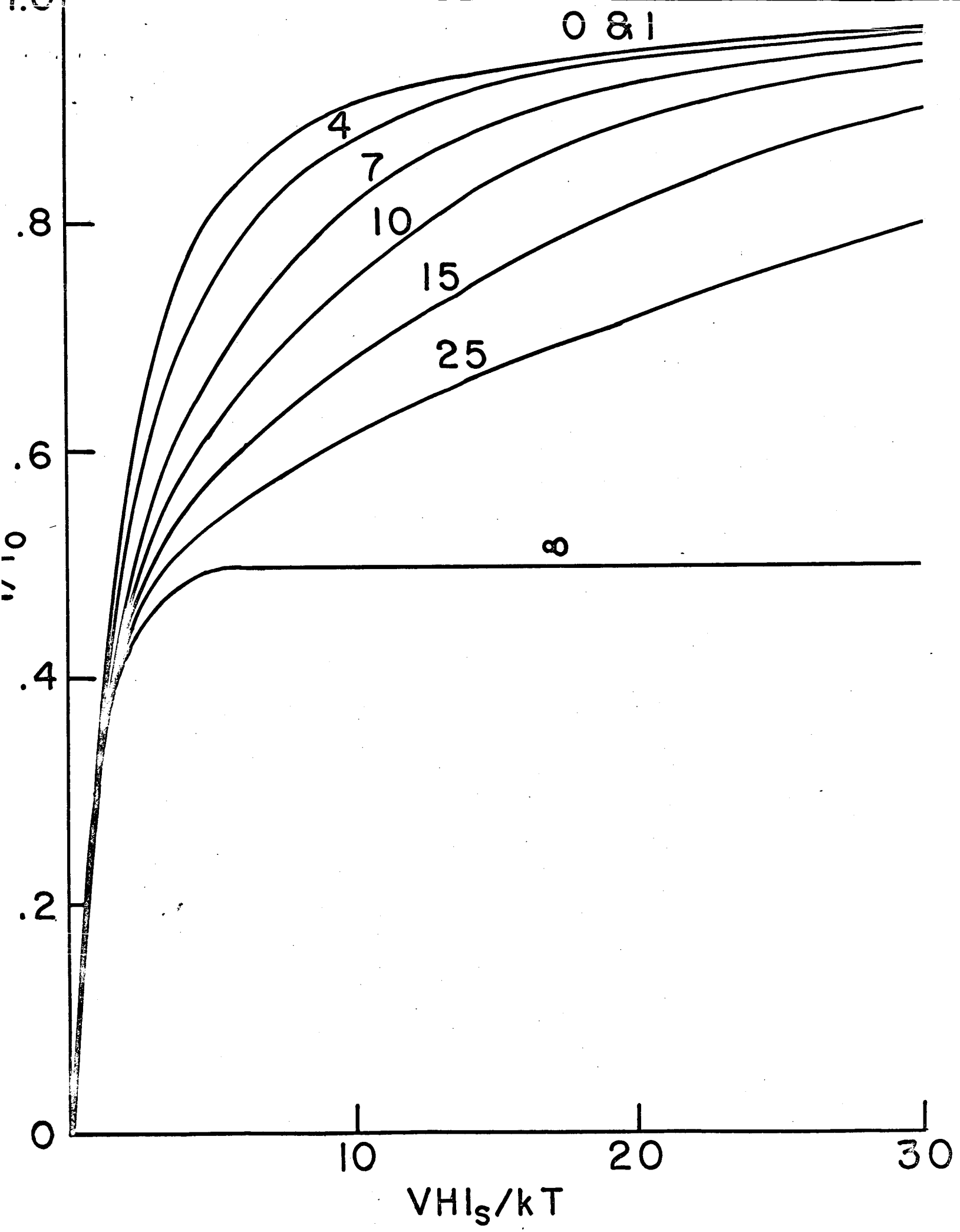
0 & 1
4
7
10
15
25
∞
1.0
.8
.6
.4
.2
0
10
20
30
VHI_s/kT

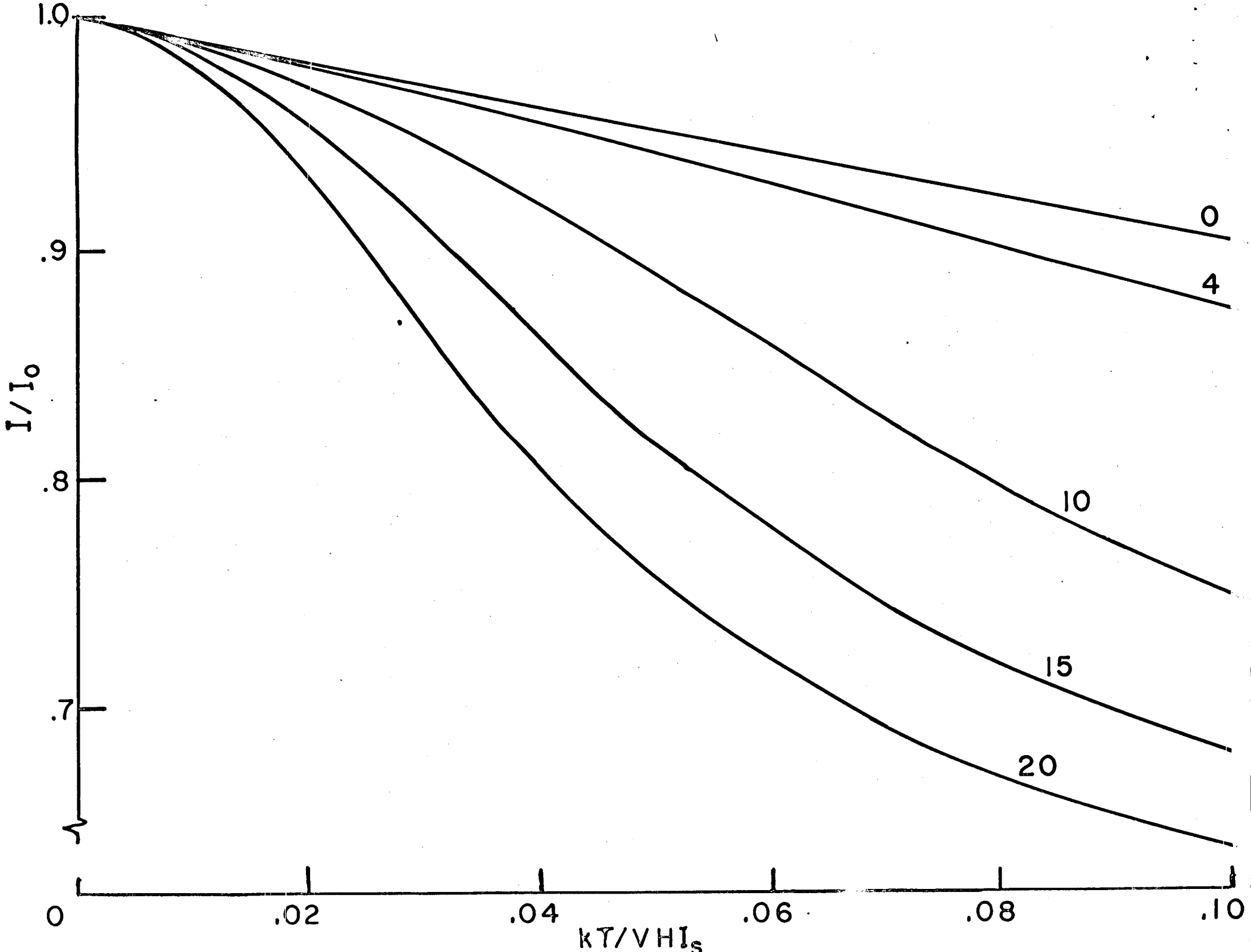
1.0
.9
.8
.7
I/I₀
0
4
10
15
20
0
.02
.04
.06
.08
.10
kT/VHI_s

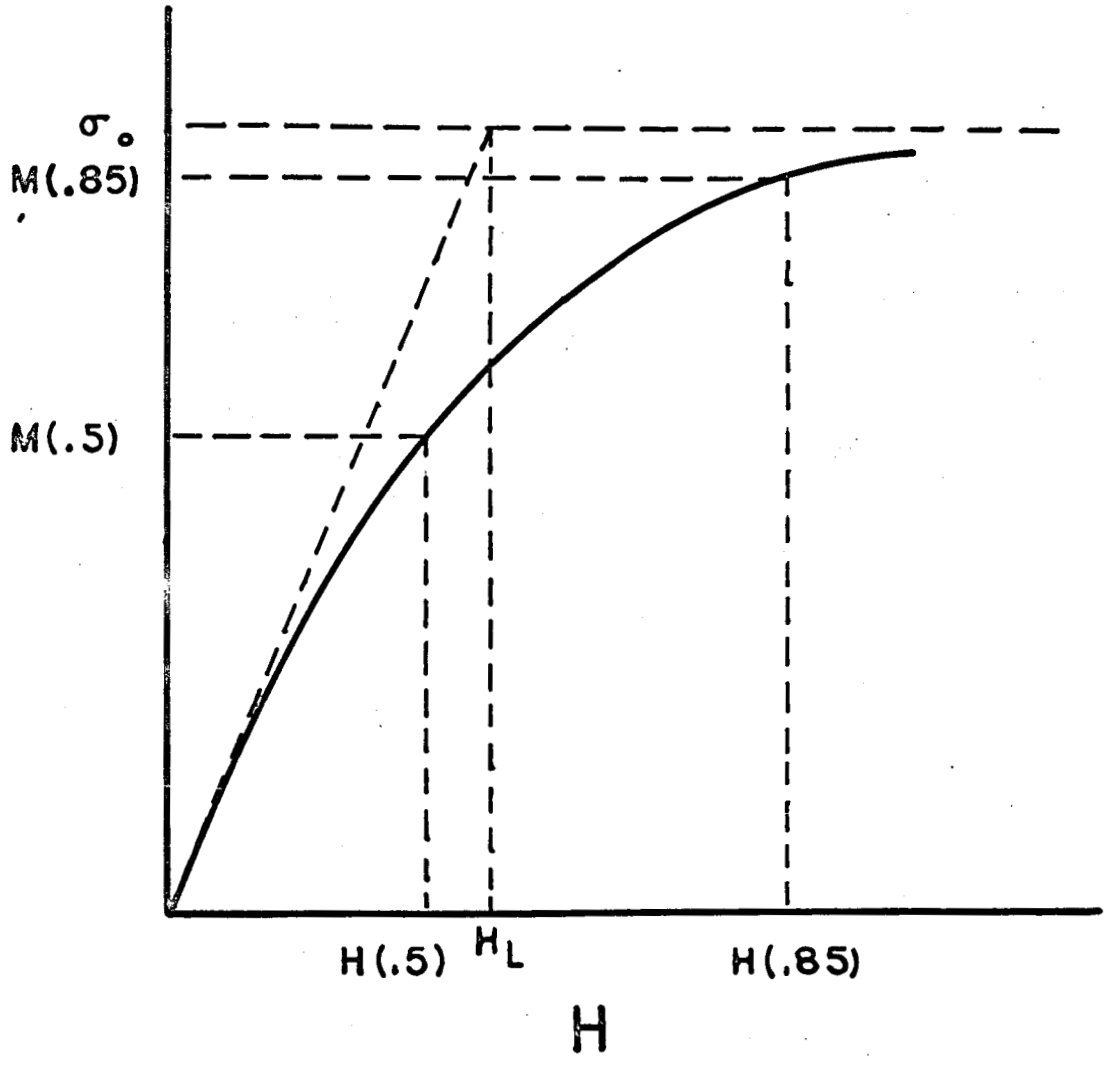
σ₀
M(.85)
M(.5)
H(.5)
H_L
H(.85)
H

Fig 6a

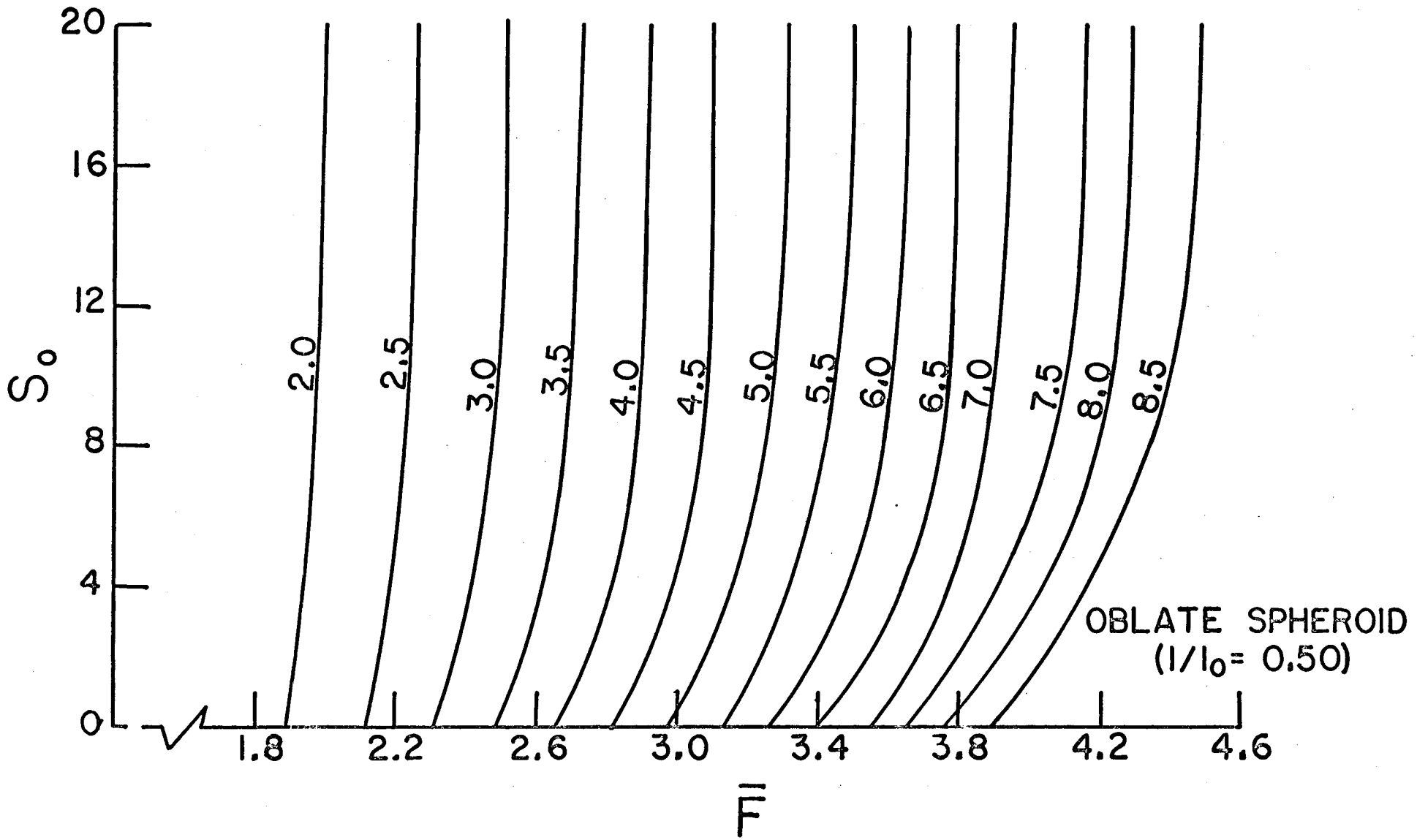
20
16
12
8
4
0
S_o
2.0
2.5
3.0
3.5
4.0
4.5
5.0
5.5
6.0
6.5
7.0
7.5
8.0
8.5
OBLATE SPHEROID
(I/I_o = 0.50)
1.8
2.2
2.6
3.0
3.4
3.8
4.2
4.6
$\bar{F}$

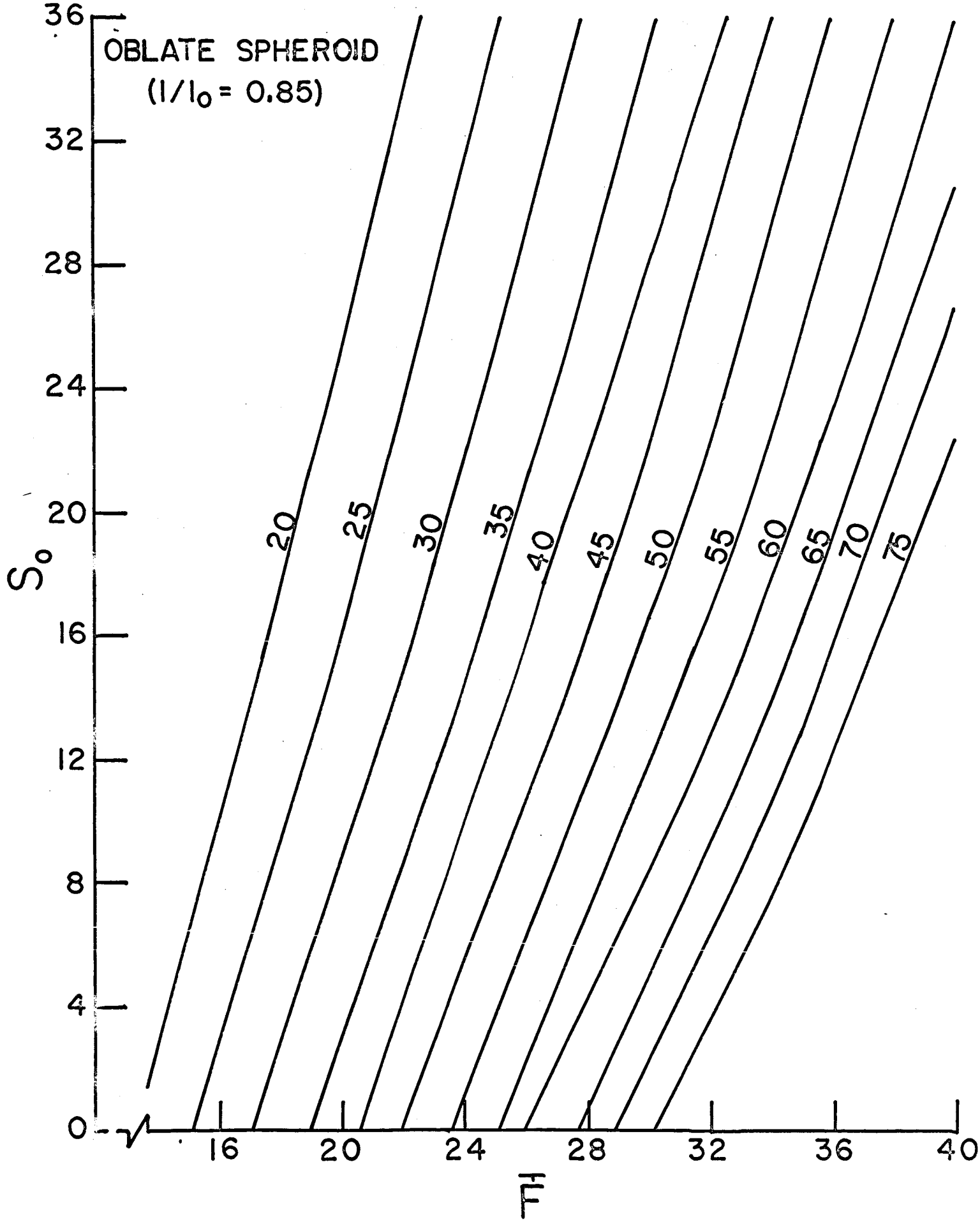

OBLATE SPHEROID
(1/l₀ = 0.85)
36
32
28
24
20
16
12
8
4
0
S₀
20
25
30
35
40
45
50
55
60
65
70
75
16
20
24
28
32
36
40
F̄

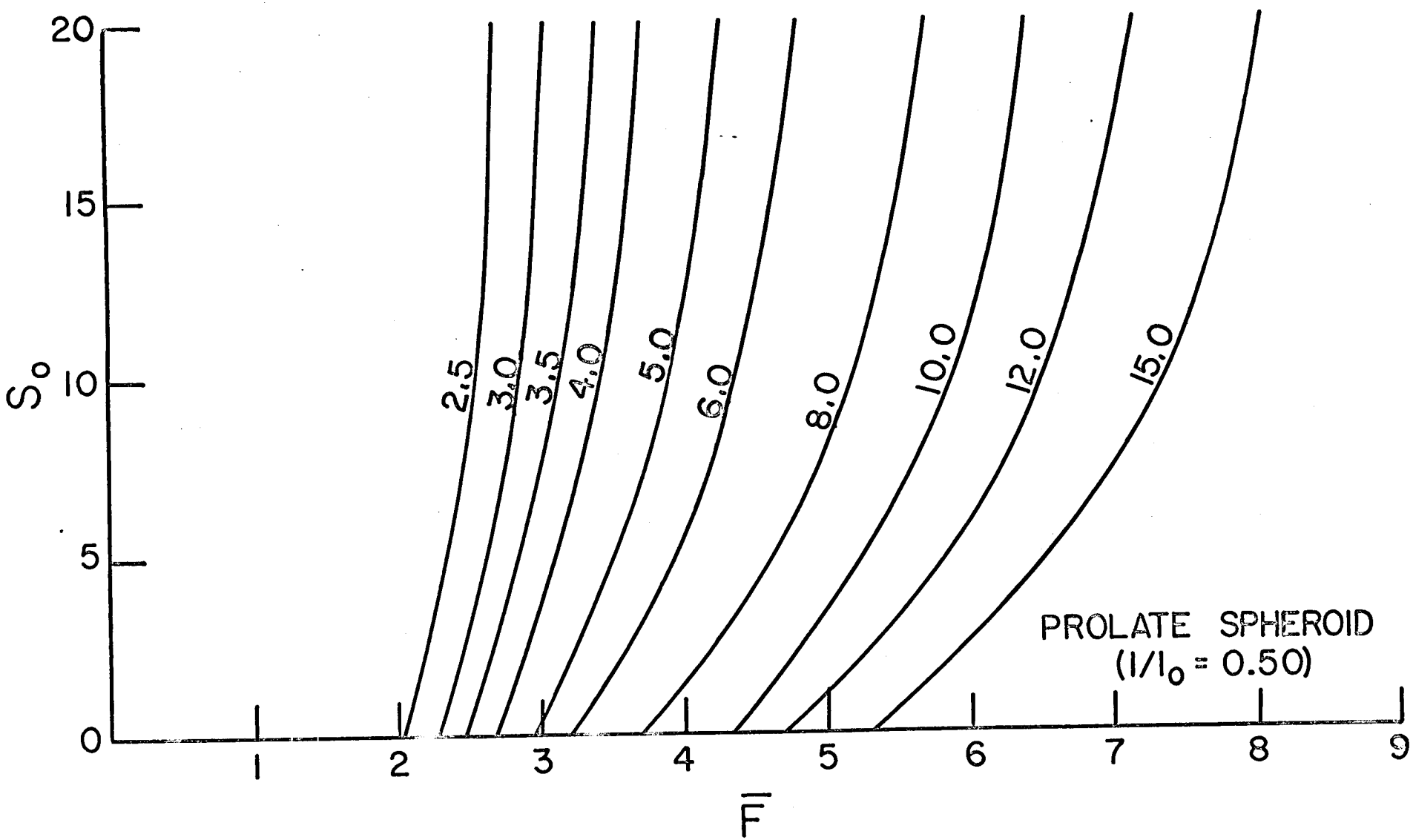
20
15
10
5
0
S_o
2.5
3.0
3.5
4.0
5.0
6.0
8.0
10.0
12.0
15.0
PROLATE SPHEROID
$(l/l_o = 0.50)$
1
2
3
4
5
6
7
8
9
$\bar{F}$

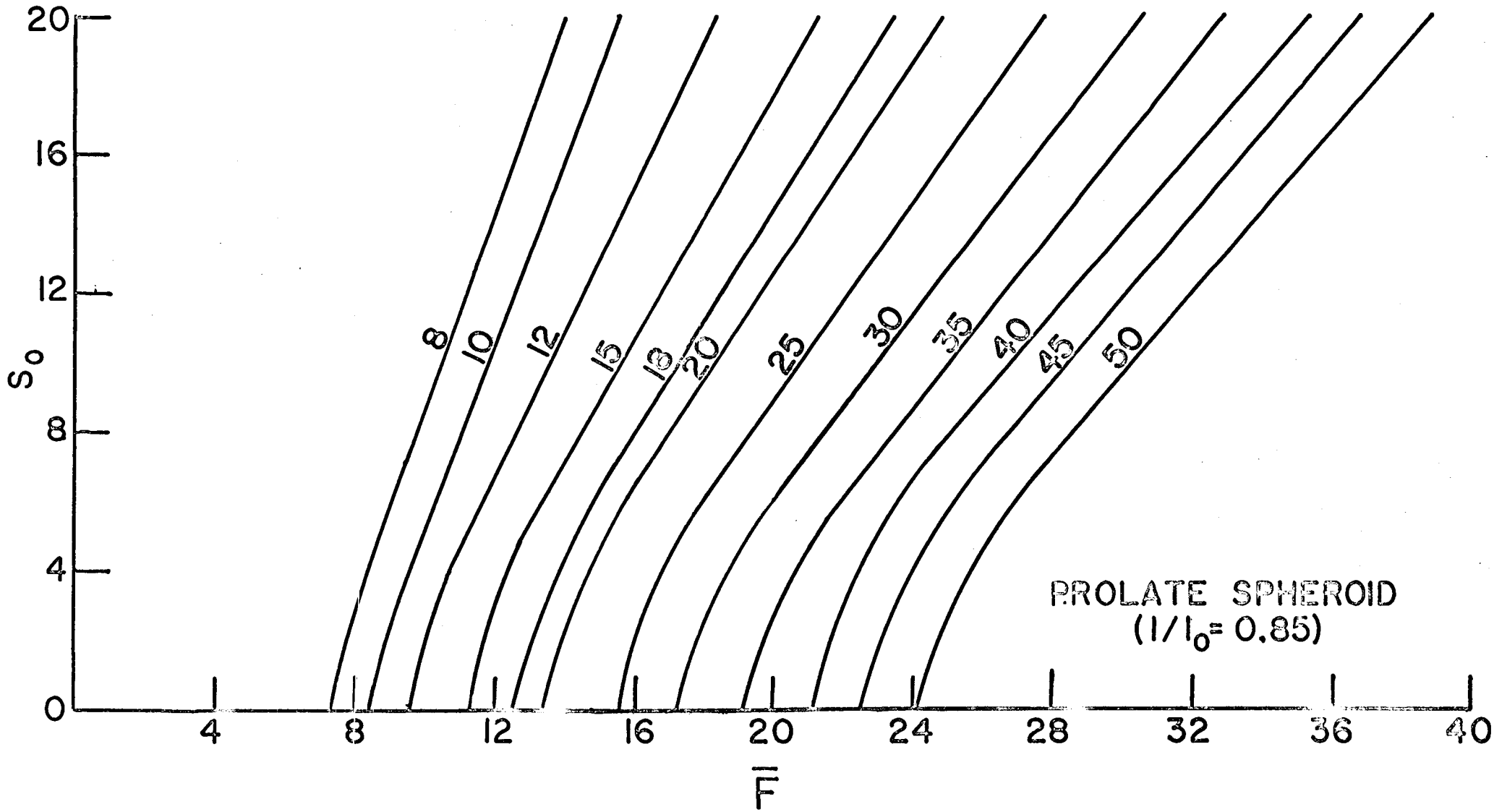
20
16
12
8
4
0
S_0
8
10
12
15
18
20
25
30
35
40
45
50
PROLATE SPHEROID
$(1/l_0 = 0.85)$
4
8
12
16
20
24
28
32
36
40
$\bar{F}$

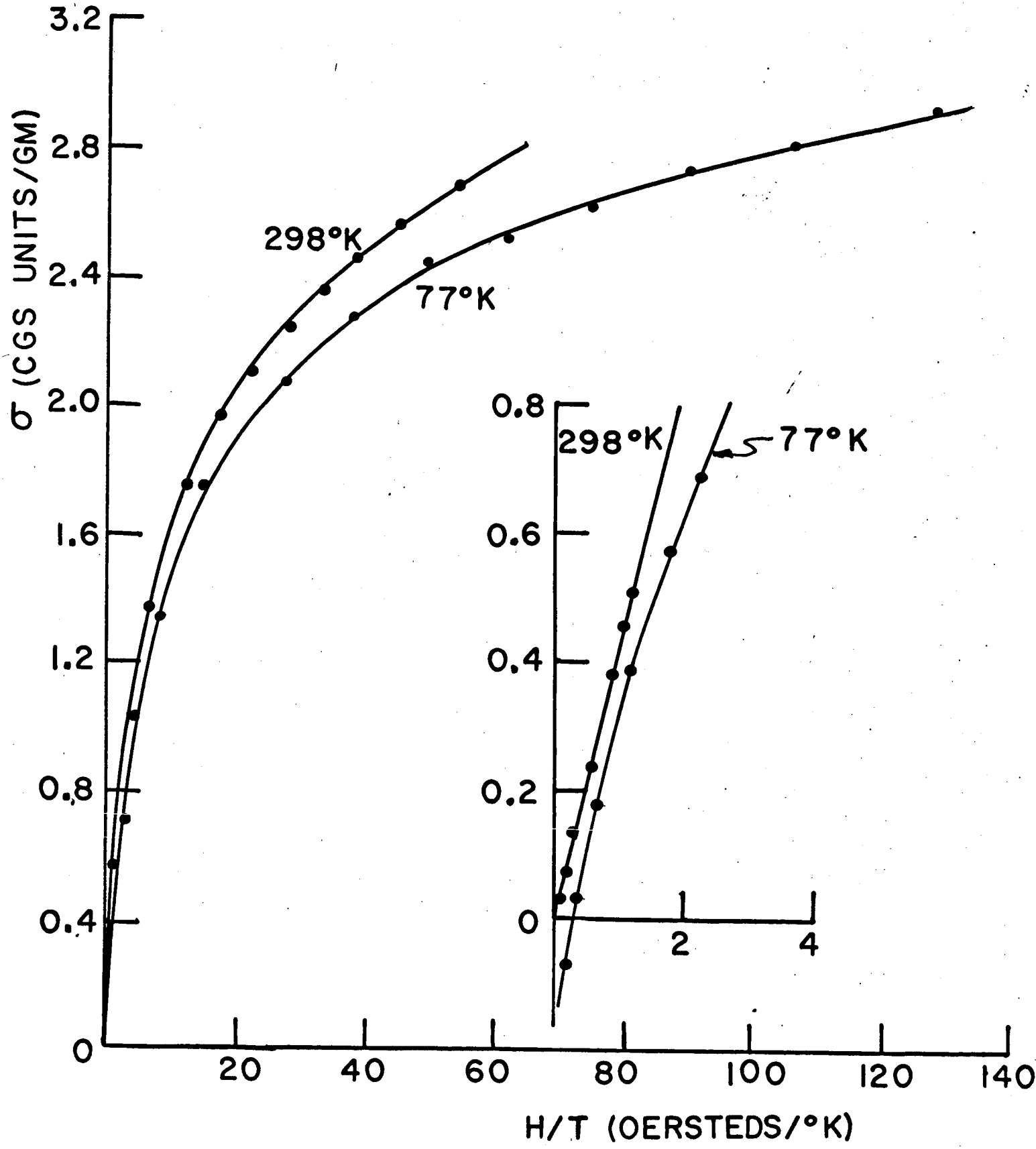
3.2
2.8
2.4
2.0
1.6
1.2
0.8
0.4
0
σ (CGS UNITS/GM)
298°K
77°K
0.8
0.6
0.4
0.2
0
2
4
298°K
77°K
20
40
60
80
100
120
140
H/T (OERSTEDS/°K)

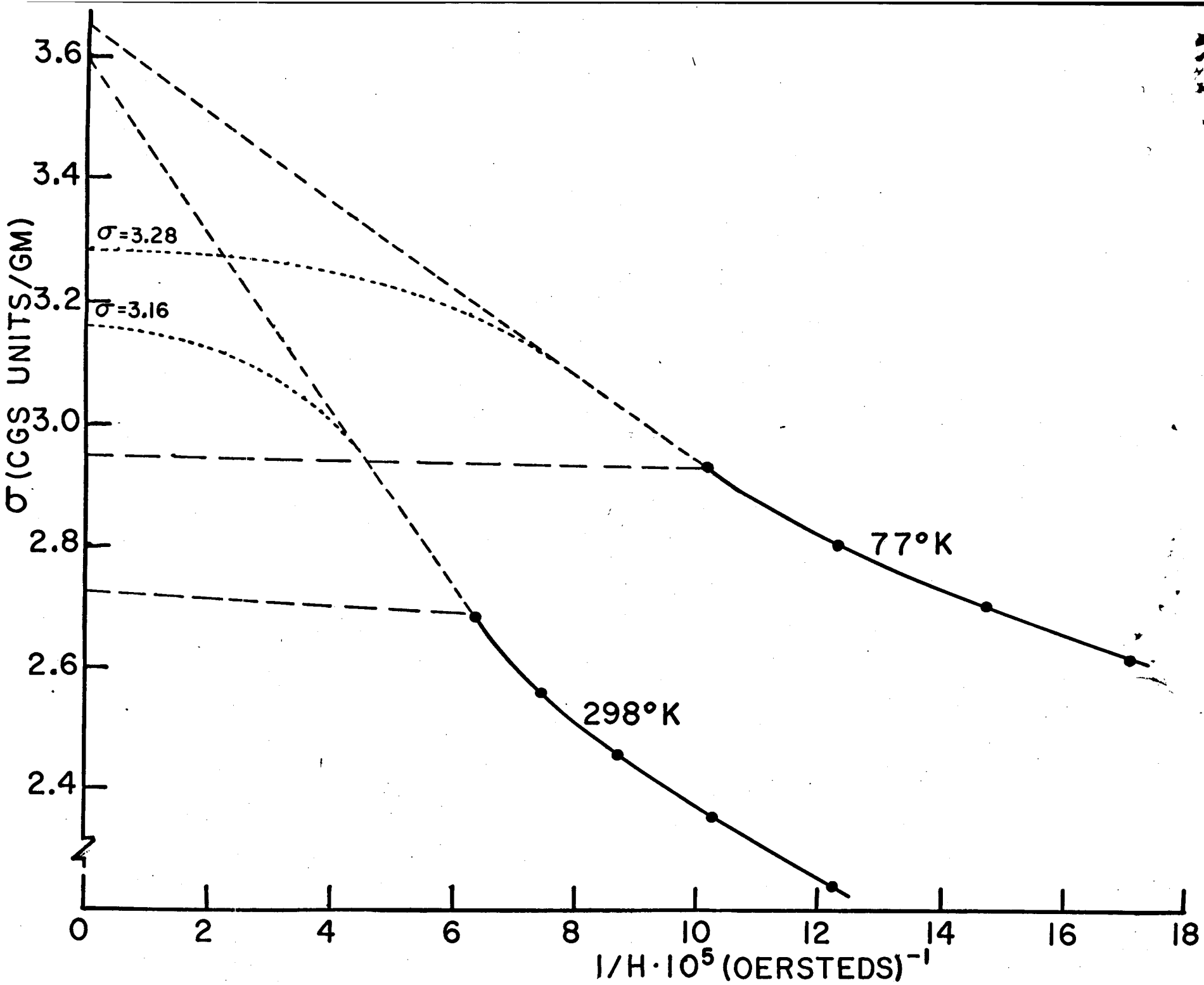
3.6
3.4
3.2
3.0
2.8
2.6
2.4
σ (CGS UNITS/GM)
σ=3.28
σ=3.16
77°K
298°K
0
2
4
6
8
10
12
14
16
18
1/H·10^5 (OERSTEDS)^-1